This is a post print of a published manuscript in the journal Construction and Building Materials, doi: https://doi.org/10.1016/j.conbuildmat.2021.122402

WEATHERING OF SERPENTINITE STONE DUE TO IN SITU GENERATION OF CALCIUM AND MAGNESIUM SULFATES

R. Navarro: r.navarro@igme.es

D. Pereira: mdp@usal.es

E. Fernández de Arévalo: e.fernandez@igme.es

E.M. Sebastián-Pardo: rolando@ugr.es

C. Rodríguez-Navarro: carlosrn@ugr.es

Accepted: 19-01-2021

Published in Construction and Building Materials

Location

- Diarium.usal.es/mdp
- Repository: University of Salamanca: https://gredos.usal.es/handle/10366/154506
- Repository: arXiv: https://eartharxiv.org/

DOI: https://doi.org/10.1016/j.conbuildmat.2021.122402

WEATHERING OF SERPENTINITE STONE DUE TO IN SITU GENERATION OF CALCIUM AND MAGNESIUM SULFATES

R. Navarro [a], D. Pereira [a,b], E. Fernández de Arévalo [c], E.M. Sebastián-Pardo [d], C. Rodriguez-Navarro[d]

[a] CHARROCK Research Group. University of Salamanca, Plaza de los Caídos s/n, 37008 Salamanca, Spain.
[b] Department of Geology, University of Salamanca, Plaza de los Caídos s/n 37008 Salamanca, Spain.
[c] Natural stone and technological tests laboratory. Spanish Geological Survey, c/La Calera 1, Tres Cantos, Madrid 28760, Spain.
[d] Department of Mineralogy and Petrology. Faculty of Sciences. University of Granada, Spain. Avda. Fuentenueva s/n 18002 Granada, Spain.

*Corresponding author (e-mail: rafanavarro74@gmail.com)

Highlights:

- Comparison of original quarry and monument samples to establish the decay mechanisms
- In situ salt formation in serpentinites under different environmental conditions
- The salt formed due to the presence of sulfides is the main cause of decay
- Identification of all the factors that act synergistically in their decay
- Measures to avoid deterioration has been proposed

Abstract

This paper presents a thorough study of the main features and the decay causes and mechanisms of serpentinites both freshly quarried and after centuries exposure at the main façade of the sixteenth century Royal Chancery (Granada, Spain). In particular, the process of in situ formation of calcium and magnesium sulfates has been studied. Several decay factors are identified, all of them acting synergistically in the deterioration of slabs made of serpentinite. Among them, the presence of sulfides such as pyrite in the original serpentinite as a result of chemical weathering induces the formation of sulfate salts such as gypsum or epsomite is considered the main cause of decay. In addition, incorrect restoration treatments involving the use of Portland cement to fill up cracks and surface lacunae, the polluted environment of the surrounding area, and the location of the slabs close to the ground, favoring capillary rise of water, all contributed to their deterioration. This work helps to gain knowledge on the deterioration process of ornaments made of serpentinite, allowing us to propose the most appropriate measures to guarantee their conservation.

Keywords: Serpentinite; sulfates; gypsum; epsomite; decay, dimension stone; heritage.

1. Introduction

Serpentinites are rocks formed by serpentine group minerals (hydrated magnesium silicates), derived from the alteration of ultramafic rocks [1,2]. They are usually traded under the common name of "Green Marble" in the industry of dimension stones due to their habitual transformation into carbonates [3,4]. They have been used as ornamental and building stones throughout history for both decorative and structural purposes. These stones were described as part of buildings in Ancient Greece, the Roman Empire [5] or Byzantium Empire [6], including cities in Hispania, such as Itálica [7] and Tarraco Nova [8] or Pre-Ottoman Islamic buildings in cities such as El Cairo (Egypt) [9,10]. From the Middle Ages, they are present in important buildings such as palaces, cathedrals, or churches throughout Europe. Some of the best examples of their use can be found in Italy, in historical buildings such as Massimo Palace (nineteenth century) or the Basilica of Saint Mary Major (fifth century), and several cathedrals all over the country (Roma, Florence, Siena or Monza) [11-16]. In South and North America, serpentinites were also used to shape decorative artifacts by Aztecs (fourteenth century) [17]. More recent examples can be found in the Havana Cathedral (eighteenth century) or in cities like Philadelphia, where the use of this material at the end of the nineteenth century was a characteristic feature of its architecture [18]. The well-known gallery of the general assembly of the United Nations in New York is characterized by its front made of serpentinites, this time coming from Val d'Aoste (Italy). At present, serpentinites are being widely used and sought mainly for its aesthetic features, existing hundreds of varieties exploited and marketed worldwide [19].

In Spain, the best known traded serpentinites are the varieties known as *Verde Pirineos* (from Galicia, NW Spain), *Verde Macael*, and *Verde Almería* (both from Andalucía, SE Spain). There was another variety, known as *Verde Granada* which was extracted in Granada (SE Spain), in Sierra Nevada. This serpentinite was discontinuously extracted from the sixteenth century to the middle of the twentieth century in several quarries, but the most important in terms of quality of the material was the quarry "Barranco de San Juan". It was used all over Spain in emblematic buildings such as the Royal Monastery of El Escorial (sixteenth century), the Royal Palace (eighteenth century) in Madrid and cathedrals such as Toledo and Jaen (seventeenth century), Cuenca and Segovia (eighteenth century), and Granada, in different periods (from sixteenth to twentieth century), among many others [20].

One of the most emblematic buildings in Granada that highlight the use of serpentinites is the façade of the Royal Chancery (Fig. 1a), which was finished in 1587 [21]. This building was the High Superior Court between 1505 and 1834 and at present is the headquarters of the High Court of Andalucía. The slabs of serpentinite used in the pedestals of columns at the front door at the main façade have an advanced state of decay, with almost fully disintegrated areas (Fig. 1b). Recent inappropriate restoration interventions involving the use of Portland cement and white marble, materials with very different physical-chemical properties and decay behavior, may have increased the deterioration, in addition to the obvious aesthetic damage.

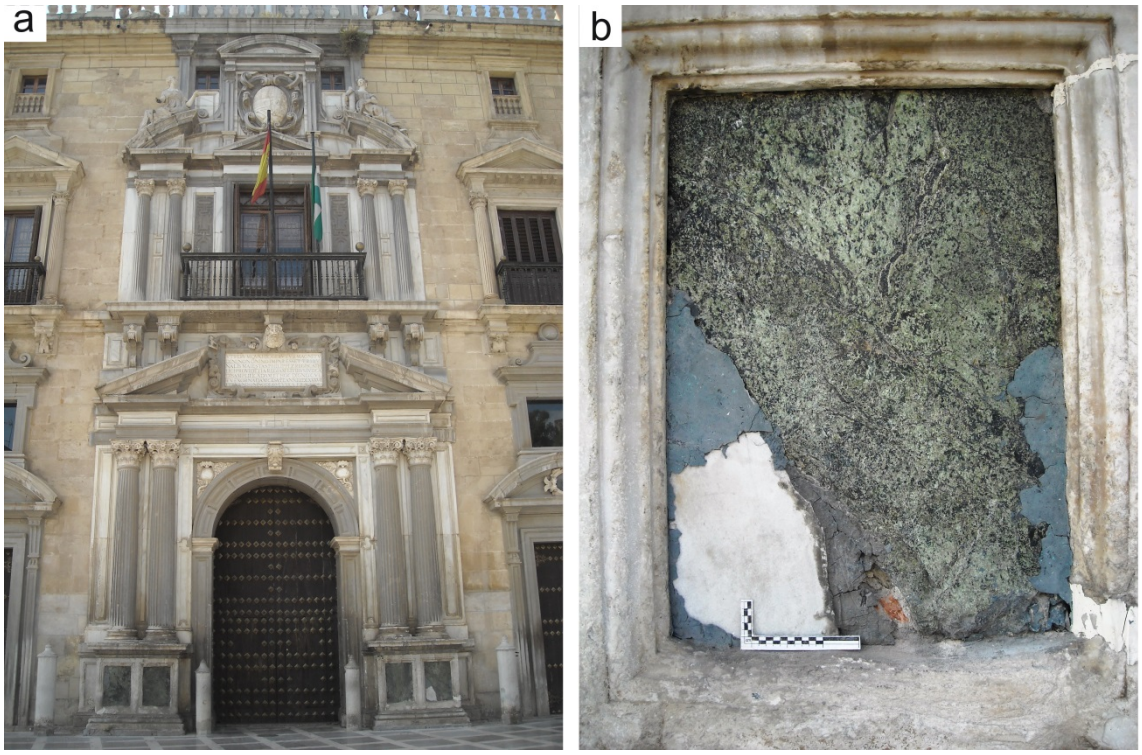

Fig. 1. a) Front view of the main door of the Royal Chancery.; b) detail of one of the serpentinite slabs conforming the pedestal of the columns and showing the advanced state of deterioration. Note the presence of Portland cement (grey patches) and a piece of white marble, used to fill lacunae. The dimensions of the slabs of serpentinite are 75 cm height and 55 cm width.

Despite a large number of studies and publications on mineralogy and serpentinization processes, there are hardly any systematic studies on serpentine as decorative and dimension stone and its decay processes in urban environments. The first studies were carried out in the early 1990s [11,12,22,23], but it was not until 2003 when a profuse number of works on this subject begun to be published [3,4,6,13-16,18,20, 24-35]. Most of these studies focused on the description of the stones used in different construction elements, as well as their location, geological features, and quarries. Very few details, however, were given about the conservation status or the pathologies affecting the stone [14,20,24,29]. Most works described the main petrographic, geochemical, and/or physical-mechanical characteristics of serpentinites in historic buildings and the original quarries, all related to their use as dimension stone [6,16,26,27,30,34]. Stone pathologies were discussed in [22], concerning the formation of salts in serpentinite and marble of the main altar of the Convent of the Descalzas Reales, in Madrid; Other authors [11,12,23,25] analyzed the main causes of damage to the serpentinites used in different buildings in Florence, Empoli, and Siena; Meierding [18] refers to the state of conservation of multiple buildings in the Pennsylvania area (Philadelphia, USA), whereas Pereira [3,28] analyzed the state of conservation and the mechanisms of alteration of serpentinite once placed in construction. Gulotta [15] studied the causes of deterioration and color changes of the serpentinite slabs used for the restoration of the façade of Monza Cathedral (Italy). Navarro [4] compared the different behavior of serpentinites depending on the degree of transformation to carbonates while in [31] were described how UV radiation affects polished serpentinite slabs.

For all the aforementioned, it is observed that, in general, there are non-exhaustive systematic studies on the alteration of serpentinites in the built heritage, and in particular on the effects of the mineralogy, texture, and composition of these stones on their alteration once they are emplaced in a building.

This work aims to determine, from the study of the Royal Chancery case, the main mechanisms of alteration of a variety of serpentinite, *Verde Granada*, which was used in numerous historical

buildings throughout Spain. A detailed characterization of the mineralogy, texture, and chemical composition of both the original quarry material and the altered material in the monument was carried out. Furthermore, through laboratory tests, the weathering mechanisms and the process of in situ formation of calcium and magnesium sulfates have been determined. This allows us to know in detail the decay problems these stones suffered and to propose the most appropriate measures to guarantee their conservation.

2. Location and geological context

The main source of serpentinites used as decorative and dimension stone in Spain was the quarry named “Barranco de San Juan”, located in Güejar-Sierra (Granada, SE Spain) (Fig. 2). Geologically, these serpentinites belong to the Nevado-Filábride Complex (NFC), which is the lowest metamorphic complex of the Internal Zones of the Betic Cordillera. The NFC is traditionally subdivided into two tectonic units, the Veleta unit (lower unit) and the Mulhacen Unit (upper unit). The stratigraphic sequence is very similar in both cases. It is composed of dark schist with quartzites (Carboniferous), quartzites, mica schist (Permian), and interlayered quartzites and schist and marbles (Permian-Triassic) at the top [36]. Interlaid in the sequence, the presence of metamorphosed igneous rocks, mainly metabasites and orthogneisses with tourmaline, is common. The metabasites, with thickness from several centimeters to hundreds of meters, are interspersed in the mica schist and marble units (Mulhacen Unit), except the "Barranco de San Juan” outcrop, which is placed in the dark schist unit (Veleta unit). According to [36], the metabasites correspond to former basic volcanic extrusions interlayered in metasediments. These metabasites are composed of amphibolites and serpentinites [37]. Fig. 2 shows the geological setting of the studied area.

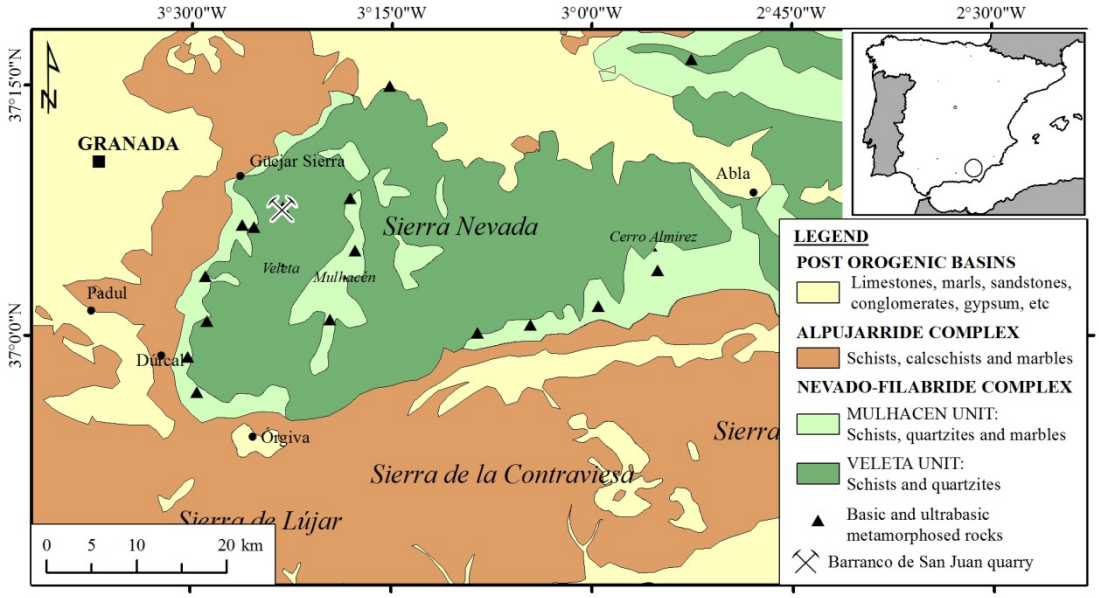

Fig. 2. Location and geological setting of the studied area (Modified from [38]).

3. Material and methodology

3.1 Samples

Two kinds of samples were collected for this work: from the “Barranco de San Juan” quarry and from the Royal Chancery building.

To characterize the main features of the serpentinites of the “Barranco de San Juan” quarry, several hand samples with similar appearance (total weight about 40 kg) were taken from the

original quarry face (Fig. 3a). These samples were cut in different sizes to get enough material for testing (Samples BSJ 1 to BSJ 5). In addition, six samples of fine-grained, apparently altered material filling fractures or precipitated in the surface, with different colors (red, yellow, brown, and white) were also collected (Fig. 3b). The different varieties observed were separated by handpicking based on color (Samples BSJ 10 to BSJ 15).

Regarding the Royal Chancery building, four samples (CHAN 1 to 4) (Fig. 3c) of different sizes (maximum 3 cm) of disaggregated material from the outer slabs placed at the bottom under the columns of the main façade were collected. No extra damage was caused to the building during this sampling.

Fig. 3. a) Field aspect of serpentinites where the quarry samples were taken; b) disaggregated alteration material close to a fractured area in the face of the serpentinite quarry; c) serpentinite samples from the Royal Chancery. The samples are scales that fell off during studying (just by gently touching the surface) due to the high level of decay.

In the Table 1 are summarized the samples used and the tests done on each sample.

Table 1. Summary of studied samples and the tests done. Abbreviations: XRD: X-Ray Diffraction; OM: Optical microscope; ICP: Inductively Coupled Plasma Analysis; MIP: Mercury intrusion porosimetry; Salt: Salt formation by capillarity suction test; FESEM: Field Emission Scanning Electron Microscopy; SO_2: determination of resistance to aging by SO_2 action in the presence of humidity

Sample	Origin	Description	Tests						
			XRD	OM	ICP	MIP	Salt	FESEM	SO_2
BSJ 1	Quarry	Hand samples of serpentinite from quarry face with different naked-eye aspect	X	X	X	X	X		X
BSJ 2			X	X	X	X			
BSJ 3			X	X	X				
BSJ 4			X	X	X		X		X
BSJ 5			X	X	X				
BSJ 10	Quarry	Green-yellow alteration sample	X		X				
BSJ 11		White alteration sample	X		X				
BSJ 12		Red alteration sample	X		X				
BSJ 13		Black alteration sample	X		X				
BSJ 14		Silky white alteration sample	X		X				
BSJ 15		Brown alteration sample	X		X				
CHAN 1	Monument	Superficial efflorescence	X		X			X	
CHAN 2		Superficial efflorescence	X		X			X	
CHAN 3		Fragment of serpentinite	X		X	X		X	
CHAN 4		Fragment of serpentinite	X		X			X	
SALT	Test	Efflorescence from Salt formation by capillarity suction test	X					X	
ACID A	Test	Efflorescence after SO2 test of BSJ 1 (Solution A)	X						

ACID B	Test	Efflorescence after SO2 test of BSJ 1 (Solution B)	X						

3.2 Analytical techniques

3.2.1 Mineralogy and chemical composition

The mineral phases of all the samples of this work were determined by means of powder X-ray diffraction (XRD) with a diffractometer *X'pert-Pro, PANalytical* (Cu Kα radiation λ=1.5405 Å; 40 kV voltage, 40 mA intensity, 4º-70º 2θ exploration range, 0.04º 2θ/s goniometer speed). The efflorescence sample generated in one of the tests (sample SALT) was analyzed with a diffractometer Phillips PW-1710 (Cu Kα λ=1.5405 Å, 40 kV voltage, 40 mA intensity, 4º-70º 2θ exploration range, 0.01º 2θ/s goniometer speed). The crystalline phases were identified with the software XPowder V.2010.01.05 Pro [39] using the PDF-2 database (International Centre for Diffraction Data).

To describe in detail the mineralogy and the textural characteristics of fresh quarry samples (BSJ 1 to 5), thin sections were studied using a Nikon Eclipse E400POL transmitted-light microscope and a Nikon Eclipse E400REF reflected-light microscope with Nikon Digital Sight D5-5M built-in digital camera.

The bulk composition of quarry and monument samples was determined by means of inductively coupled plasma with optical emission spectrometry (ICP-OES). A Horiba Scientific ICP-OES Ultima 2 model was used.

3.2.2 Mercury intrusion porosimetry

For the characterization of the porous system, a Micromeritics Autopore III model 9410 porosimeter was used. One sample from the historical building (CHAN 3) and two quarry samples (BSJ 1 and 2) were analyzed (three replicate measurements per sample). For the monument sample, a 5 cm^3 solid sample penetrometer with a stem volume of 0.376 cm^3 was used, while for the quarry samples, a 15 cm^3 solid sample penetrometer with a stem volume of 0.392 cm^3 was used. The contact angle between mercury and the sample was established at 130º. The equilibration time used between each measurement point was 10 s and the maximum intrusion range was established up to a pressure value of 44500 psia. Prior to analysis, the samples were carefully washed with deionized (DI) water and oven-dried at 110ºC for 24 h.

3.2.3 Salt formation by capillarity suction test

This test was carried out to disclose the possible source of alteration of the studied serpentinite material both in the quarry and in the monument. This test simulates the possible formation of salts when the rock is affected by a continuous supply of water, as sometimes occurs in the basal areas of walls affected by capillary rise. Four parallelepipeds, two from BSJ_1 and two from BSJ_4, 2.5 x 2.5 x 8 cm in size from original quarry material were tested.

The samples were placed in a tray with a grid so that they were partially immersed in DI water (conductivity less than 15 μS cm^{-1}), under constant *T* and relative humidity (RH) conditions (19ºC and 60% RH). The objective of this test was to determine the salt formation capacity of the material, without the contribution of external agents. The samples were kept under these conditions until the formation of efflorescence was observed, which occurred after 60 days. The pH of the solution was controlled during the test with a Hannah piccolo plus Hi1295 pH-meter. This test does not follow any EC regulation. It is self-defined.

3.2.4. Field Emission Scanning Electron Microscopy with Energy Dispersive X-Ray Spectroscopy (FESEM-EDS)

The Royal Chancery samples, as well as the efflorescence generated by the capillarity suction test, were analyzed in detail to disclose their textural and compositional features. A Leo Gemini 1530 Field Emission Scanning Electron microscope (FESEM) coupled with Oxford Inca 200 Energy Dispersive Spectroscopy (EDS) microanalysis was used. Samples were C coated prior to analysis.

3.2.5. Test for the determination of resistance to aging by SO_2 action in the presence of humidity

This test measures the relative resistance of natural stone to damage caused by SO_2 in a wet environment. It aims to simulate the behavior of the material in a polluted atmosphere similar to that existing in some urban areas. This test has been carried out following the UNE-EN 13919: 2003 Standard [40]. Although this standard is currently voided, it still represents a valid test procedure in research, since the results are comparable to those coming out from a large number of similar tests used in related studies [41].

This test has been carried out on six polished quarry samples (BSJ 1 and 4) with dimensions of 12 x 6 x 1 cm, following the Standard. As a previous step, they were polished with a 1200 grit SiC paper, cleaned with DI water, and oven-dried at 70 ± 5 ºC for 48 h. Subsequently, before introducing them into the containers, they were immersed in DI water for 24 h at 20ºC. The samples were placed in hermetically sealed containers with a volume capacity of 8 liters. Two different solutions were used. In solution A, 80 ml of sulfurous acid (H_2SO_3) were diluted in 24 ml of DI water, while in solution B, 24 ml of H_2SO_3 were diluted in 80 ml of DI water. The solution was placed at the bottom of each container and the samples (3 samples per solution type -A or B-) were placed on a rack, 100 mm above the dissolution. The containers were closed and maintained at a constant temperature of 25°C. One reference test piece was left untested. After 21 days, the observed alterations (i.e., efflorescence, exfoliation, peeling, and loss of edges) were evaluated and the resulting mass loss was determined after washing the samples with DI water and oven-drying at 70ºC for 24 h. The mass loss was determined according to the equation:

$$\Delta m = \frac{(m_0 - m_i)}{m_0} x100 \qquad (1)$$

where m_0 is the mass (g) of the dry specimen before the test; m_i is the mass (g) of the dry piece after the test, and Δm is the variation of the mass (%). The newly formed efflorescence (*samples Acid A and Acid B*) was analyzed by XRD.

4. Results

The results of the XRD analysis of all samples, including the efflorescence formed in the capillarity suction test and in the SO_2 aging test, are shown in Table 2:

Table 2. Phases identified by XRD. Abbreviations according to [42] except Alu: Alunogen; Eps: Epsomite; Hal: Halotrichite; Hex: Hexahydrite; Mel: Melanterite; Moo: Moorhousite; Pck: Pickeringite; Roz: Rozenite; Slv: Slavickite.

	Atg	Mag	Mgs	Dol	Tr	Py	Cal	Tlc	Chr	Qz	Slv	Roz	Mel	Pck	Hal	Eps	Alu	Clc	Gp	Hex	Moo
BSJ 1	X	X	X			X															
BSJ 2	X			X	X	X	X	X													
BSJ 3	X			X	X	X	X	X													
BSJ 4	X	X																			

	Atg	Mag	Mgs	Dol	Tr	Py	Cal	Tlc	Chr	Qz	Slv	Roz	Mel	Pck	Hal	Eps	Alu	Clc	Gp	Hex	Moo
BSJ 5	X								X												
BSJ 10										X	X	X	X								
BSJ 11														X	X	X					
BSJ 12															X		X				
BSJ 13						X				X				X	X			X			
BSJ 14								X										X			
BSJ 15								X		X				X		X		X			
CHAN 1	X									X									X		
CHAN 2	X						X												X		
CHAN 3	X	X																			
CHAN 4	X	X																			
SALT	X	X																	X		
ACID A																			X	X	X
ACID B																X			X	X	

With regard to the fresh quarry samples (BSJ 1 to BSJ 5), the main phase detected was serpentine (probably antigorite; the determination of the actual polymorph, which is nontrivial, was out of the scope of this paper) with a small amount of magnetite or carbonates (magnesite, dolomite and/or calcite) and chromite or pyrite. In addition, BSJ 2 and BSJ 3 samples, showed the presence of tremolite, talc, and pyrite. As for the altered quarry material (samples BSJ 10 to 15), XRD analysis revealed the presence of numerous hydrated sulfates such as slavikite (Na, Mg, Fe), rozenite and melanterite (Fe), pickeringite (Mg, Al), halotrichite (Fe, Al), epsomite (Mg), and/or alunogen (Al), along with quartz, talc or clinochlore. Fig. 4 shows some XRD patterns of the different samples analyzed.

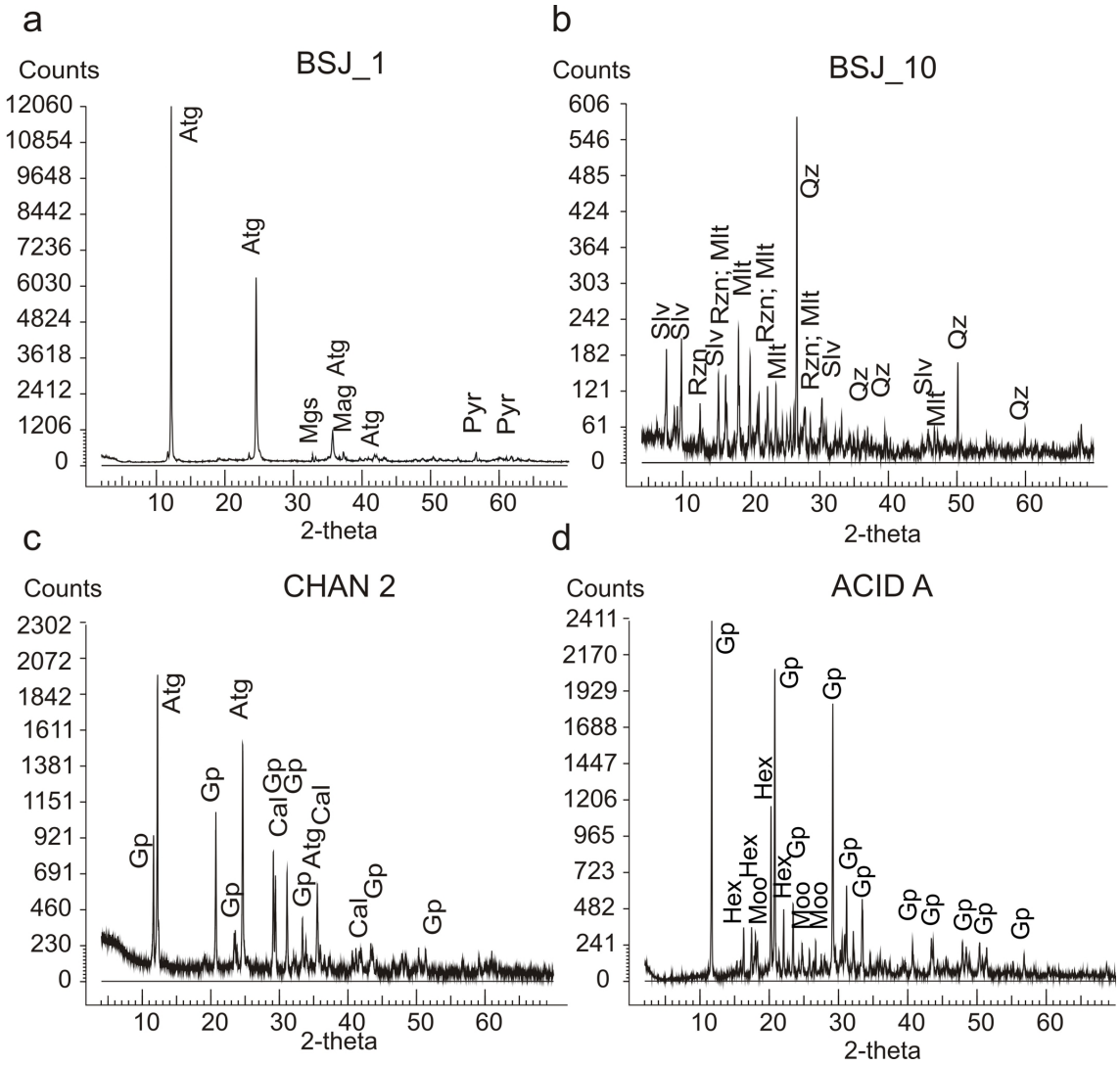

Fig 4. XRD patterns of samples: a) BSJ 1; b) BSJ 10; c) CHAN 2

In thin section, serpentine (antigorite) is the main mineral phase observed in all cases. Olivine, pyroxene, amphibole, chlorite, carbonates, fibrous serpentine (chrysotile), and opaque minerals were observed as accessory minerals. The latter minerals were identified as magnetite, ilmenite, chromite, pyrite, and sphalerite by reflected light. The secondary minerals are carbonates, mainly magnesite and calcite or dolomite, as well as talc and hematite, as previously identified by XRD. In samples BSJ 2 and BSJ 3, serpentine (antigorite) stands out along with carbonates, while as accessories opaque (magnetite, pyrite) and amphibole (tremolite), chlorite, garnet, with some oxides as secondary minerals were also observed. The main observed texture was non-pseudomorphic interpenetrating texture [43], with areas of pseudomorphic texture in which some minerals remain from the original rock, or only the shape of the porphyroblasts (bastites), are still conserved. A fracture fill texture was also observed, composed of chrysotile and carbonates, and sparse acicular amphiboles. Fig. 5 shows different aspects of the studied samples.

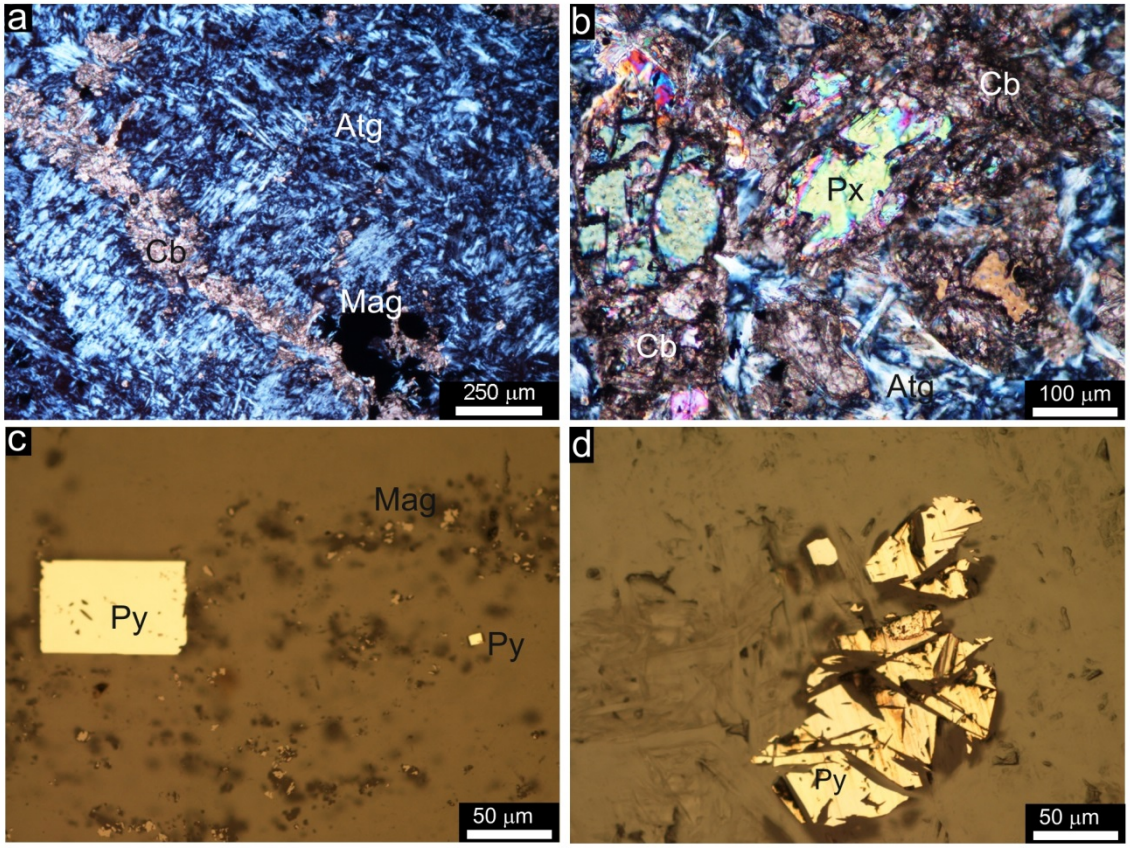

Fig. 5. Photomicrographs of samples from the quarry. a) fracture filling with carbonates (Cb) and magnetite (Mag) in a matrix of serpentine (Atg) with non pseudomorphic interpenetrating texture (sample BSJ 1; transmitted light; crossed nicols); b) pyroxene (Px) partially transformed to carbonates and antigorite, with non pseudomorphic interpenetrating texture (sample BSJ 2; transmitted light; crossed nicols): c) pyrite (Py) crystals with disperse magnetite (Mag) (sample BSJ 1; reflected light; crossed nicols); d) Anhedral pyrite (Py) crystal (sample BSJ 4; reflected light; crossed nicols).

The XRD analysis of the Royal Chancery samples showed serpentine minerals (antigorite) along with other phases such as gypsum, quartz, and calcite, together with magnetite.

Regarding the efflorescence samples, XRD analysis showed that gypsum was formed after the capillary suction test, whereas efflorescence formed after the SO_2 aging test included gypsum and hexahydrite. It is noteworthy that in the case of Solution A, a hydrated sulfate such as moorhousite (Co, Ni, Mn) was also detected together with the two salt phases above indicated.

Table 3 shows the major elements analyzed by ICP-OES:

Table 3. Major elements detected by ICP-OES. (*) Below the detection limit. (+) Not determined (due to lack of sufficient sample).

Sample	SiO_2 %	Al_2O_3 %	MgO %	CaO %	Fe_2O_3 %	K_2O %	MnO %	Na_2O %	P_2O_5 %	TiO_2 %	SO_3 %	LOI %
BSJ 1	42.12	1.31	35.17	0.15	9.41	0.03	0.06	0.01	0.00	0.01	*	11.78
BSJ 2	23.04	0.33	24.67	20.24	3.63	0.00	0.12	0.03	0.00	0.01	4.39	23.02
BSJ 3	24.10	0.63	27.13	17.01	3.63	0.01	0.11	0.03	0.00	0.01	4.12	22.31
BSJ 4	39.19	1.92	39.43	0.86	7.54	0.01	0.09	0.01	0.00	0.01	*	11.52

BSJ 5	40.05	1.85	39.42	0.16	6.50	*	0.09	0.01	0.00	0.01	*	12.62
BSJ 10	20.28	5.84	15.34	0.04	3.52	0.32	0.60	0.20	0.04	0.31	26.26	26.25
BSJ 11	2.71	11.08	0.69	1.05	5.52	0.11	0.22	0.01	0.02	0.24	37.57	40.73
BSJ 12	3.82	10.04	9.11	0.06	2.44	0.07	0.17	0.06	0.01	1.96	37.65	32.42
BSJ 13	13.01	8.03	14.61	0.06	3.28	0.10	0.14	0.12	0.03	2.30	36.70	22.50
BSJ 14	60.14	0.55	2.16	0.02	31.67	0.03	0.03	*	0.01	*	*	4.48
BSJ 15	32.55	11.67	4.53	0.75	7.19	0.65	2.86	0.13	0.40	0.32	20.09	19.06
CHAN 1	31.30	2.31	5.47	0.08	29.30	9.50	0.47	0.32	0.06	0.02	1.90	20.10
CHAN 2	21.70	1.85	4.05	0.05	17.00	13.00	1.60	4.25	0.01	*	2.77	+
CHAN 3	38.09	2.58	9.76	0.11	38.49	0.51	0.20	0.18	0.03	*	*	+
CHAN 4	40.51	0.96	6.19	0.08	37.40	0.95	0.05	0.03	0.01	0.03	*	13.84

The major elements of quarry samples reflect a composition in accordance with the mineralogy of the studied serpentinites. The quarry samples can be subdivided into two groups. Samples BSJ 1, BSJ 4, and BSJ 5 showed that silica and magnesium oxide were the two predominant compounds, also being in similar proportions. Iron oxide is the third in terms of weight percentage. The oxide of aluminum and the oxide of calcium are also present, which do not reach 1 wt%, the same as other oxides such as manganese or titanium. The second group included the samples with more mineralogical variety as observed by XRD and optical microscopy (i.e., BSJ 2 and BSJ 3). In this case, silica, magnesium oxide, and calcium oxide were the three most abundant oxides, but with a notable increase in calcium oxide content in detriment of magnesium oxide. A decrease in the iron oxide content and an increase in volatile material were also noted. It is noteworthy the presence of sulfur trioxide in BSJ 2 and BSJ 3 samples, which as corroborated by XRD and optical microscopy could be in the form of sulfides (pyrite). Weathered quarry samples (BSJ10 to BSJ 15) include a large amount of sulfur trioxide, with all samples above 19 wt% and reaching in some cases 37 wt% , consistent with the presence of sulfates as secondary weathering products (XRD results). The high content of volatile material, over 20 wt%, is consistent with the fact that, as indicated above, most of these samples include hydrated iron-oxyhydroxides and magnesium sulfates.

In general terms, the monument samples show an overall composition consistent with that of the quarry serpentinites, but some differences were observed, especially in samples CHAN 1 and CHAN 2. . Sample CHAN 1 shows a decrease in the content of silica and magnesium oxide, as compared to the quarry samples, and a significant increase in the content of calcium oxide, sulfur trioxide, and volatile material, which is indicative of the presence of hydrous phases such as gypsum and antigorite. This is also observed in the case of sample CHAN 2, which is mainly composed of salts. In this case, in addition to the important content of calcium oxide and sulfur trioxide, the presence of other characteristic salt-related alkali elements such as potassium and sodium stands out. These elements could be present in the form of sulfates and/or nitrates or carbonates. The other samples analyzed, CHAN 3 and CHAN 4, have a composition very similar to the fresh samples collected in the quarry, consistent with XRD results. There are, however, significant variations in the iron oxide content, which might be due to differences in magnetite or other iron oxides content. An increase in potassium oxide and sodium oxide content was also observed, which may again be indicative of the presence of salts.

Table 4 shows the results of the mercury intrusion porosimetry (MIP) analysis. The quarry samples showed a low connected (or open) porosity, ranging between 0.88% and 1.59%, while the analyzed sample of the Royal Chancery had a much higher porosity (3.44%), about two to four times that of the quarry samples. As for the values of aparent or skeletal density, there are hardly any noticeable differences between the three samples. As for the average pore radius, in the case of the Royal Chancery sample, a notable increase was observed as compared to the quarry samples.

Table 4. Characteristics of the porous system by MIP of samples from the quarry and the Royal Chancery. Average values and standard deviation are indicated.

Sample	Pore volume (cm^3/g)	Total porosity (%)	Apparent density (kg/m^3)	Skeletal density (kg/m^3)	Average pore radius (mm)	Pore total area m^2/g
BSJ 1	0.0028±0.004	0.88±0.10	2714±4	2692±4	0.036±0.12	0.353+0.176
BSJ 2	0.0060±0.0018	1.59±0.47	2678±16	2635±12	0.037±0.015	0.737±0.737
CHAN 3	0.0130±0.002	3.44±0.54	2745±15	2650±13	0.075±0.005	0.690±0.110

Regarding the pore size distribution (PSD), when analyzing the graph (Fig. 6) it was observed how the curves of the three samples show a bimodal PSD, with a large amount of pores in the largest and smallest sizes and less in the intermediate size range. While the BSJ 1 sample had a slightly higher percentage of macropores than micropores, both the BSJ 2 sample and the CHAN 3 sample had a higher proportion of pores with a size <2.5 μm. In all cases, most pores (approximately 90%) are below 100 μm in size.

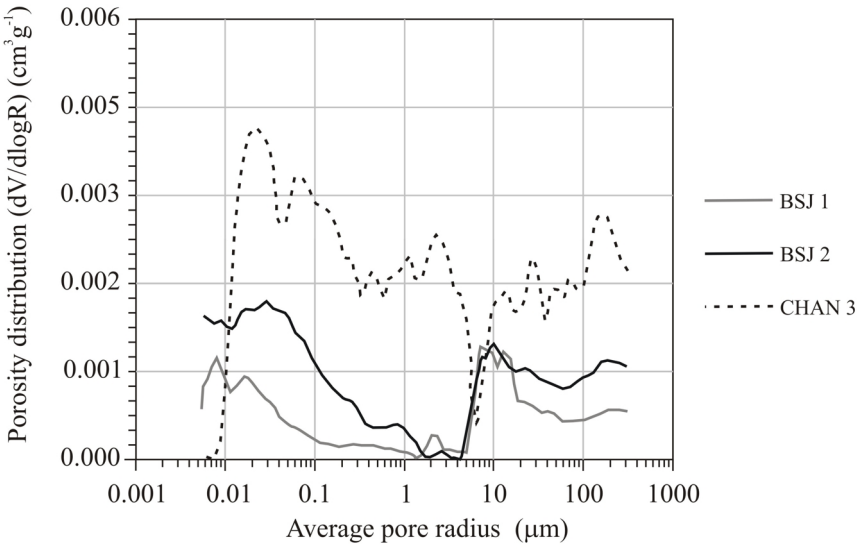

Fig. 6. Pore size distribution of samples from quarry and monument.

Regarding salt formation by capillarity suction, this test was performed to determine if the source of the efflorescence observed both in the quarry and the monument was the serpentinite itself or an external source. Sixty days after the partial immersion of the samples in deionized water, the presence of efflorescence was observed in one of the samples (Fig. 7a-c). Efflorescence was especially concentrated on a fracture that was filled with chrysotile fibers. XRD showed that the efflorescence was mainly made up of gypsum (Table 1), along with serpentine minerals (antigorite) detached from the substrate due to salt crystallization (see below).

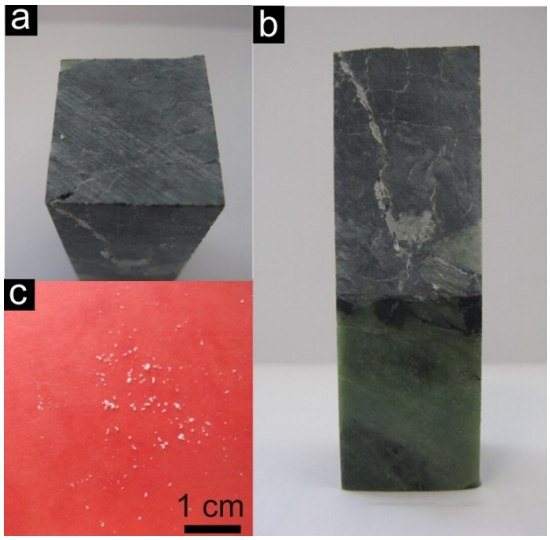

Fig. 7. a) View of the serpentinite block where the saline efflorescence was generated; b) Lateral view of the fracture in which efflorescence was developed; c) collected efflorescence sample.

FESEM analysis of the efflorescence showed bulky aggregates attached to chrysotile fibers and antigorite plate-like crystals according to EDS analysis (Fig. 8a). When the bulky aggregates were studied in detail (Fig. 8b), an incipient state of alteration was observed, evidenced by the development of new saline phases (e.g. gypsum) in the holes of the antigorite aggregates (Fig. 8c). EDS analysis showed the presence of S, Cl, K, Na, and Ca, in addition to Si, Mg, and Al, characteristic of serpentine. The presence of Fe was detected in grains also containing S, indicative of the residual presence of pyrite, or without S in some crystals, possibly magnetite, which could not be clearly distinguished.

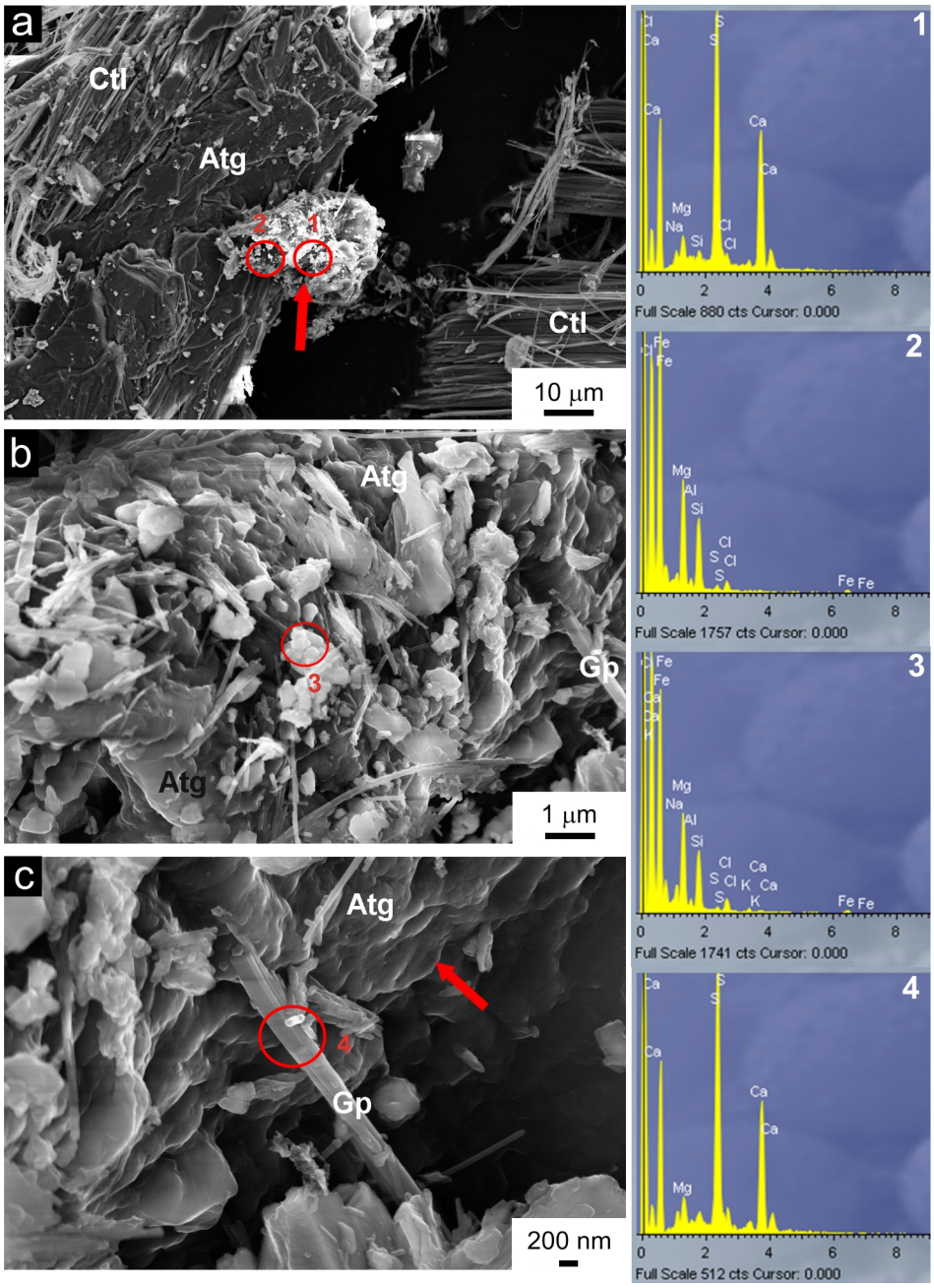

Fig. 8. FESEM images and EDS analysis of SALT sample: a) view of a crystalline aggregate adhered to antigorite (Atg) crystals, which contains gypsum and magnetite, among other salt phases not clearly identified; b) detail of the crystal aggregate in (a), showing the development of fine gypsum crystals (Gp) in the corrosion pits of antigorite. Note the corroded appearance of the antigorite crystals in contact with gypsum; c) detail of one of these gypsum crystals and the corrosion marks (red arrow) developed on the antigorite crystal. The numbers correspond to the EDS analysis.

Concerning the samples of the Royal Chancery, it was observed that practically the entire sample was covered by salts, especially gypsum (Fig. 9a and b), along with other phases such as calcite and epsomite (Fig. 9c), identified by EDS analysis.

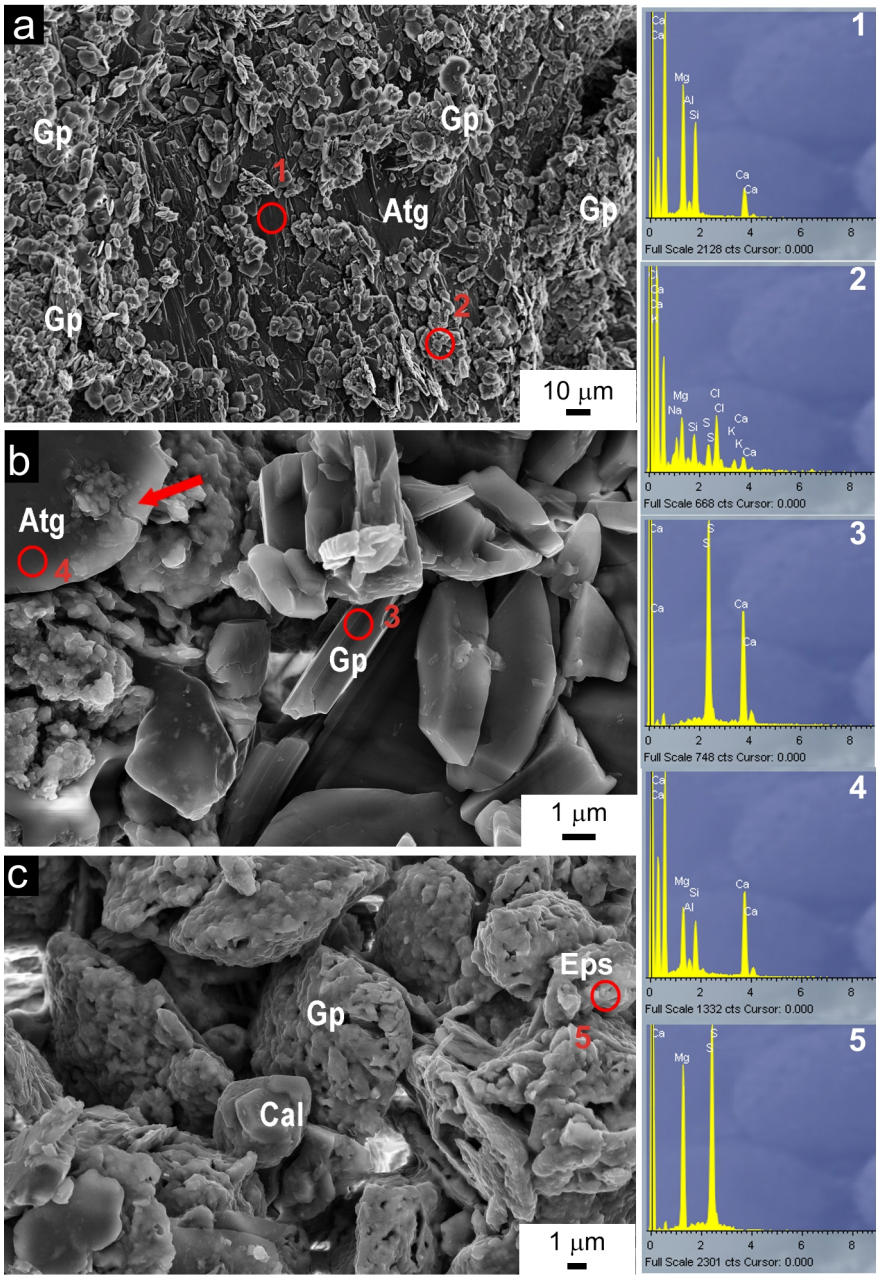

Fig. 9. FESEM images and EDS analysis of the samples of the Royal Chancery (CHAN 1): a) general view of the sample where it is possible to observe how gypsum (Gp) covered almost all the surface; b) breakdown of an antigorite (Ag) crystal (red arrow) due to the precipitation of cryptocrystalline gypsum; c) gypsum corroded by dissolution processes, together with calcite (Cal) and epsomite (Eps) crystals. The numbers correspond to the EDS analysis.

The weight loss after carrying out the SO_2 test was below 1%, being somewhat higher in solution A, with a higher concentration of SO_2 (Table 5). Regarding the superficial changes, in addition to the formation of efflorescence (Fig. 10a), the main alterations observed were color changes due to oxidation (Fig. 10b), dissolution in fractures (Fig 10c), and fracture and loss of surface material. In this case, scaling was not observed, as [22] documented in the case of the serpentinites of the Monasterio de las Descalzas Reales in Madrid.

Table 5. Weight loss after the SO_2 test.

Sample	Solution A Weight Loss (%)	Solution B Weight Loss (%)
BSJ 1	0.098	0.061
BSJ 4	0.295	0.156

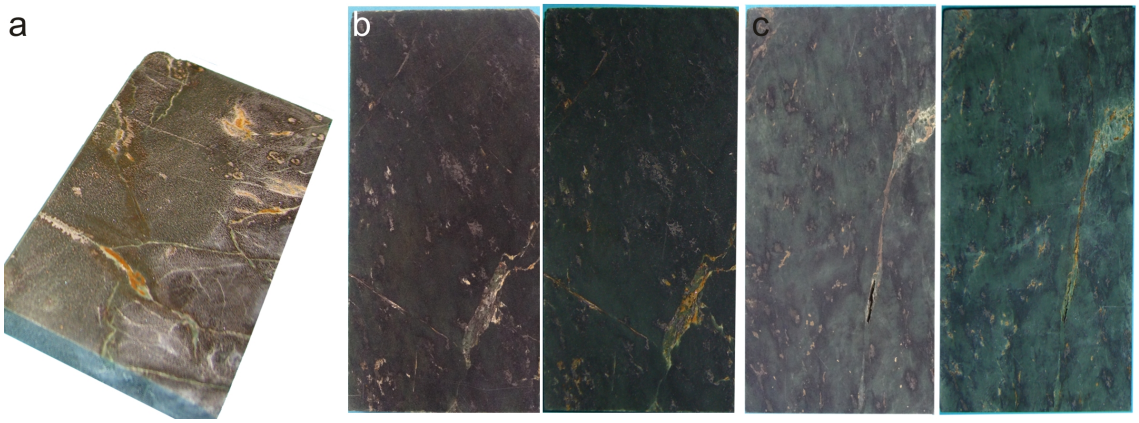

Fig. 10. a) Sample BSJ 1: efflorescence, especially highlighted near a fracture; b) Sample BSJ 1: left: before the test; right: after the test; c) Sample BSJ 4: left: before the test; right: after the test. It is noteworthy the color changes and the loss of material through the fractures; c). Width of each piece: 6 cm.

5. Discussion

The presence of sulfides, such as pyrite or sphalerite, in serpentinites, is widely documented [44-49]. In the case of the serpentinites of the "Barranco de San Juan" quarry, Arana-Castillo [50] revealed the presence of these sulfides, detected both by XRD and in thin section. Regarding the phases observed in the alteration materials taken from the quarry face (BSJ10 to BSJ15), they are characteristic of secondary alteration products of sulfides in supergene environments [51], especially iron sulfides (pyrite), following their oxidation and hydrolysis in the presence of water. The oxidation of pyrite in the presence of water, together with minerals rich in magnesium and calcium, such as those from the serpentine or carbonate group (magnesite, calcite or dolomite), can induce the formation of calcium or magnesium sulfate salts, mainly gypsum and epsomite. In addition, other iron sulfates such as melanterite or pickeringite [52] can be formed, commonly precipitating as efflorescence [53,54]. The pyrite oxidation process follows the (simplified) evolution shown below. The initial reaction would be [52]:

$$FeS_2 + H_2O + 7/2O_{2\,(aq)} \rightarrow Fe^{2+} + 2SO_4^{2-} + 2H^+ \quad (1)$$

where for each mole of oxidized pyrite, 2 moles of hydrogen (H^+) are generated, which implies, therefore, a decrease in the pH of the medium.

The Fe^{2+} released in reaction (1) can be subsequently oxidized according to:

$$Fe^{2+} + H^+ + 1/4\ O_{2\,(aq)} \rightarrow Fe^{3+} + 1/2\ H_2O \quad (2)$$

This reaction consumes part of the acidity generated by pyrite dissolution. The generated Fe^{3+} can, in turn, promote the oxidation of pyrite according to the reaction:

$$FeS_2 + 14Fe^{3+} + 8H_2O \rightarrow 15Fe^{2+} + 2SO_4^{2-} + 16H^+ \quad (3)$$

After the oxidation of pyrite, the released Fe^{2+} can be oxidized (2), or it can precipitate forming secondary phases such as melanterite or pickeringite-halotrichite, among others. Some of the occurring reactions are [52]:

$$Fe^{2+} + SO_4^{2-} + 7H_2O \rightarrow Fe^{2+}SO_4 \cdot 7(H_2O) \quad \text{(melanterite)} \quad (4)$$

$$Fe^{2+} + 2Al^{3+} + 4SO_4^{2-} + 22H_2O \rightarrow Fe^{2+}Al_2(SO_4)_4 \cdot 22(H_2O) \quad \text{(halotrichite)} \quad (5)$$

$$Mg^{2+} + 2Al^{3+} + 4SO_4^{2-} + 22H_2O \rightarrow MgAl_2(SO_4)_4 \cdot 22(H_2O) \quad \text{(pickeringite)} \quad (6)$$

$$Mg^{2+} + SO_4^{2-} + 7H_2O \rightarrow MgSO_4 \cdot 7(H_2O) \quad \text{(epsomite)} \quad (7)$$

$$Ca^{2+} + SO_4^{2-} + 2H_2O \rightarrow CaSO_4 \cdot 2(H_2O) \quad \text{(gypsum)} \quad (8)$$

When $CaCO_3$ is present in sulfide-containing serpentinites undergoing weathering, acidity is neutralized, and oxidation of Fe^{2+} to Fe^{3+} occurs rapidly [55], iron precipitates, and calcium and sulfate bind to form gypsum, according to the reaction [56]:

$$Fe^{3+}_{(aq)} + 2SO4^{2-}_{(aq)} + H^+_{(aq)} + 2CaCO_{3\,(s)} + 5H_2O \rightarrow Fe(OH)_{3\,(s)} + 2CaSO_4 \cdot 2H_2O_{\,(s)} + 2CO_{2\,(g)} \quad (9)$$

However, when magnesium carbonates are present, epsomite or other intermediate sulfate phases rich in magnesium will occur, depending on the temperature and humidity conditions [41]. In the case of dolomite, the reaction is as follows:

$$CaMg(CO_3)_2 + 2SO_2 + 9H_2O + O_2 \rightarrow CaSO_4 \cdot 2H_2O + MgSO_4 \cdot 7H_2O + 2CO_2 \quad (10)$$

The presence of melanterite, halotrichite, pickeringite, or epsomite, along with other similar phases that are formed as a by-product of the oxidation of pyrite or other sulfides, was also observed on the original serpentinite quarry face.

In the case of the salts (mainly gypsum) formed after the capillarity suction test, their origin could be found in the residual presence of pyrite. In conjunction with water and atmospheric O_2, the oxidation and hydrolysis of pyrite generated an acidic medium that facilitated the dissolution of other components, such as carbonates or antigorite, as was observed by FESEM-EDS (i.e., presence of corrosion pits on the serpentine minerals). This dissolved material eventually precipitated, forming salts, such as gypsum and/or epsomite.

Furthermore, after the aging test in an acidic atmosphere, very similar sulfate phases were observed such as epsomite, hexahydrite, and moorhousite. The presence of elements such as Cl, K, and Na in the efflorescence could be due to the formation of small salt crystals that were not clearly identified by FESEM. The origin of such elements is likely due to their presence in trace amounts in the water used in the test.

All in all, our results confirm that the presence of sulfides, such as pyrite, in these rocks, even in small amounts, plus the presence of polluted environments can jointly be the main sources of sulfate generation (gypsum or epsomite) in the samples of the Royal Chancery, and therefore, the main factors of decay to take into account. All these salt phases are very sensitive to changes in

relative humidity and temperature, in such a way that small variations in environmental conditions can induce phase transitions and associated salt damage [57], especially in the case of magnesium sulfates [58]. Fig. 11 shows the relative humidity (RH%) vs. temperature (*T*) phase diagram of the systems involved in this alteration: the $MgSO_4$ + H_2O system, showing the hydration-dehydration transitions of epsomite, hexahydrite and kieserite [59]; the $CaSO_4$ + H_2O system, showing the hydration-dehydration of gypsum- anhydrite [60]; and the $FeSO_4$ + H_2O system, showing the phase transition of melanterite-rozenite [61].

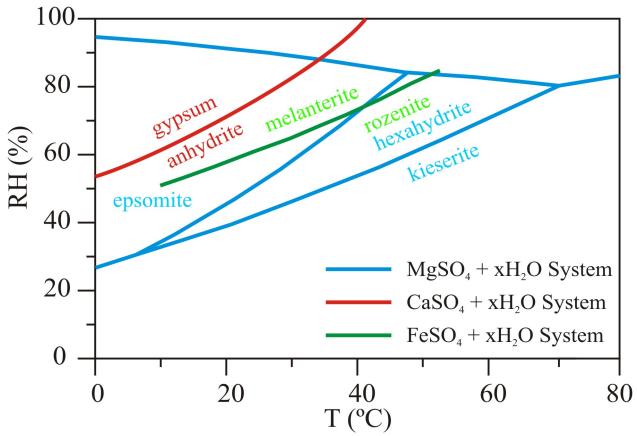

Fig. 11. RH% vs. *T* phase diagram (at 1 atm P) of the $MgSO_4$ + H_2O (modified from [59]), $CaSO_4$ + H_2O (modified from [60]) and $FeSO_4$ + H_2O (modified from [61]) systems.

This phase diagram shows that RH variations of between 40% and 80% at 23ºC will cause phase changes between different salts such as epsomite, hexahydrite and kieserite, anhydrite and gypsum or rozenite and melanterite. These phase changes can result in significant crystallization pressure, which will cause strong stresses within the stone pore system leading to its physical weathering [57,60,62]. Under certain conditions, crystallization pressure could potentially overcome the tensile strength of most stone material, leading to their fracturing and damage [62-65]. Therefore, the abundant sulfate salts formed in serpentinites such as gypsum, hexahydrite or epsomite, due to both intrinsic factors (in situ oxidation and hydrolysis of sulfides) and environmental pollution (wet and dry deposition of SO_2, followed by acid-promoted dissolution of the serpentine minerals leading to the formation of sulfate salts [66,67]) can generate high crystallization pressures inside the stone with small variations in the environmental conditions of RH and *T* such as those that occur in the day/night or summer/winter. This cyclic and repeated phase transitions, and the associated crystallization pressure generation will lead to the extensive deterioration of the serpentinite observed in the Royal Chancery.

All of the above is more evident when there is a difference between the porosity values of the samples from the quarry and the sample from the Royal Chancery. It is remarkable the increase in connected porosity that the latter has suffered. The distribution of pore sizes, although also bimodal, was less marked than in the quarry samples and much more asymmetric, highlighting a large number of pores <2.5 μm in size that had been developed. This increase in porosity could be interpreted, in the case of pores > 2.5 μm, as an effect of the crystallization of salts inside the stone resulting in crack development. Nonetheless, the majority of salt crystals filled the smaller pores. Yu and Oguchi [69] indicated that pores 0.1 to 5 μm in radius seems to be the most effective in salt absorption, while pores larger than 5 μm were not generally filled with salts. These authors observed that rocks with substantial amounts of pores about 0.1–5 μm in radius interconnected with a greater amount of smaller pores <0.1 μm in radius are very susceptible to salt crystallization damage and that the smaller pores (<0.1 μm) were important in inducing higher crystallization pressure whereas relatively large pores (i.e. capillary pores 0.1 to 5 μm in size) were more effective in salt uptake. When a critical supersaturation is reached following evaporation, crystallization will then take place in the smaller pores, not necessarily in the larger ones as

predicted by thermodynamics, because the remaining solution will be drawn by capillary forces into the smallest pores were crystallization will occur [62]. This can create tensile stresses on the surface of the pores resulting in fractures which imply that the two walls of the fracture move perpendicularly away from the fracture plane (mode I fracture opening) [69], producing micro-fracturing as well as extension and widening of pre-existing microfractures and pores [65]. Concerning the increase in the amount of pores <2.5 μm in size, which was most prominent in weathered serpentinite from the Royal Chancery, this could be explained by the dissolution of the serpentine minerals (antigorite) due to the effect of acid attack not just due to sulfide phases oxidation and hydrolysis, but also, as indicated above, to dry and wet deposition of SO_2 in the polluted environment where this monument is located (i.e., the city center of Granada, with intense traffic and residential heating) resulting in H_2SO_4 generation and acid-promoted weathering of the serpentinite minerals (both silicates and carbonates) ([66,67]). According to Teir *et al.* [70], the presence of acids such as H_2SO_4 at 1M concentrations can produce the dissolution of more than 20% of Mg and 12% of Fe, in serpentinite with a particle size of 74-125 μm, in one hour, at 20ºC. The interaction of both magnesium and iron with sulfate-containing water can lead to the formation of saline efflorescence such as epsomite, melanterite, or rozenite, as was detected in the original quarry samples during the present study. In serpentinites, the dissolution reaction due to SO_2 attack is [70]:

$$3H_2O + 3SO_2 + 3O_2 + Mg_3Si_2O_5(OH)_4 \rightarrow 3Mg^{2+} + 3SO^{2-}{}_4 + 2SiO_2 + 5H_2O \quad (11)$$

Whilst acid concentrations used in the test are significantly higher than the acid concentration in the atmosphere, the long term exposure of these stones to a polluted environment can favor their decay via the above reaction (11) [18].

As stated above, the weathering of sulfide minerals such as pyrite will also contribute to the production of secondary sulfate salts, which in turn creates the damage observed hereafter the capillary test performed using fresh quarry serpentinite. Similar weathering processes are also expected to take place in the Royal Chancery upon access of humidity to the porous system of the serpentinite.

Altogether, these processes of dissolution and fracturing cause an increase in porosity and existing pore radii, as well as the generation of new smaller pores, more reactive due to the increase in surface area that this phenomenon entails. As a result, the transport of water through the porous system is facilitated, triggering the easiness for decay. In addition to the acid dissolution of the serpentine minerals, it should be considered that the dissolution of the carbonates would also cause the generation of micropores. Although carbonates are minor phases, their high rate of dissolution in an acid medium [71] would favor this type of weathering phenomenon.

Other alterations observed after the aging test in an acid atmosphere, such as the color changes on the surface of the serpentinites, were already described by [18] in the serpentinites from the region of Philadelphia or by [15], in the case of the Cathedral of Monza (Italy). Meierding [18] justified the yellowing of the green rock due to the oxidation of the iron-rich olivine and the chromite to limonite. This yellow material frequently formed a surface crust (<2mm) due to surface precipitation of dissolved ions from inside the rock. In many cases, this author found that this layer was detached, finding a much more porous and altered serpentinite underneath, showing granular disintegration, scaling, fracturing, and chipping [72], which caused an early deterioration of the blocks. However, Gulotta [15], indicated that these discolorations are due to a loss of magnesium, at a depth of approximately 500 μm and amorphous SiO_2 surface precipitation, which becomes more evident as the rock presents more discontinuities, which also was highlighted by Bralia *et al.* [12].

In addition, it is also fundamental for the deterioration of the pieces of the monument the involvement of inadequate restoration actions (Fig. 12a and b), in which white marble and

Portland cement were used as replacements. They constitute an almost inexhaustible source of sulfates and calcium, along with magnesium from the serpentinites. Rainwater penetrates, either directly through fractures, from the contact surface with the mortar or by capillarity. Once in the porous structure of the serpentinite, water can reacts with the serpentinite minerals, but also with the carbonates and sulfates from the overlying limestone, the slabs-fixing mortar, the white marble pieces placed in previous restorations, and the Portland cement used to seal fractures. All these steps supply the necessary components for the formation of salts such as gypsum, which precipitates inside the porous structure of the serpentinite. It is important to point out that this intervention should not be the main cause of deterioration. It was done once the damage to the serpentinite slabs was very advanced, that is, once large fragments had been lost, which were replaced by white marble and Portland cement.

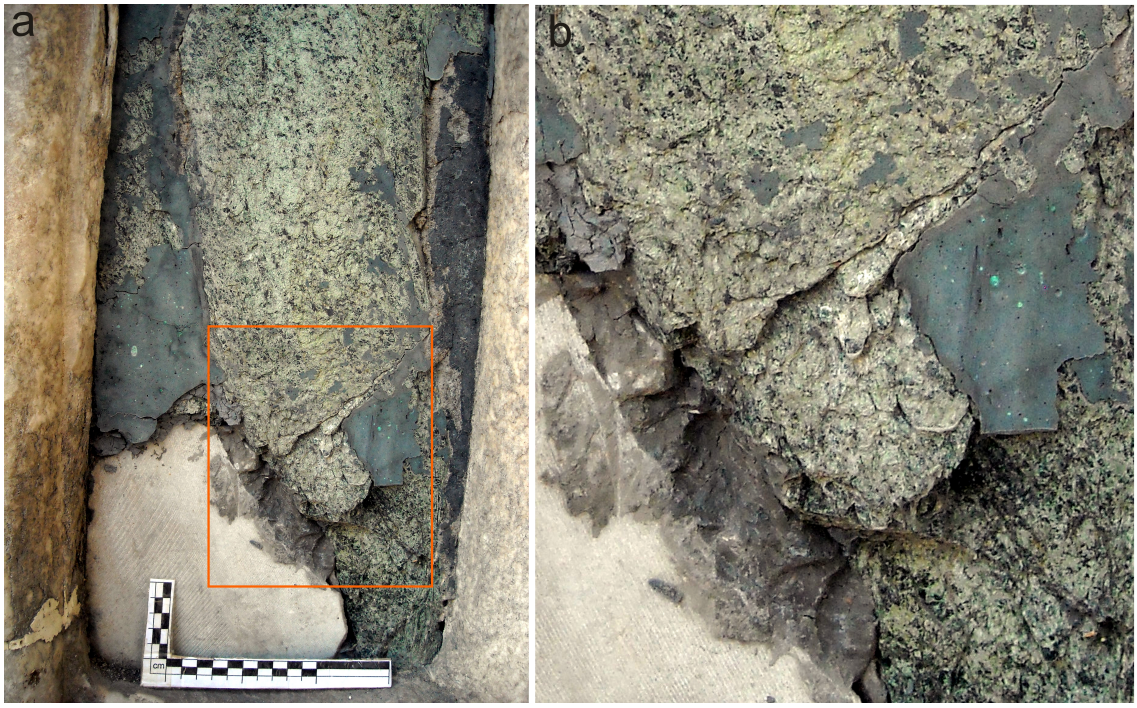

Fig. 12. a) one of the slabs that was "restored" with white marble and Portland cement; b) detail of this slab where it is possible to show the fractures and the scales.

This phenomenon of gypsum and epsomite formation can be further exacerbated by cation exchange processes between Ca-Mg from serpentinites in waters rich in calcium sulfate, as described Blanco-Varela *et al.,* [22] for the case of serpentinites in the Monasterio de las Descalzas Reales (Madrid, Spain).

Also, its emplacement close to the ground contributes to increased deterioration. The serpentinite slabs of the pedestals of the columns have a greater contribution of water, mainly by capillarity, which would also explain the greater deterioration suffered by the calcareous stones of the ashlars and the limestones (calcarenite from Santa Pudia quarry) of the columns at the bottom. Despite the low porosity of the serpentinites (up to 3.44%), compared to the calcarenite from Santa Pudia (~ 25%) with which the ashlars are made [73], the smallest pore size of the former makes the capillary front to reach greater heights. Besides this, the presence of the river "Darro", close to the square where this building is placed, causes an increase in humidity in this area. This fact has already been highlighted by Meierding [18] in the Philadelphia serpentinites, in which he observed that the greatest deterioration occurred in blocks near the ground, where the humidity was greater, regardless of the location with respect to the contribution of pollutants (rural or urban environment), and protection against rain (cornices or eaves).

Conclusions

To determine the behavior of serpentinites against the action of decay agents such as salt precipitation, humidity, and/or acid attack, a set of accelerated weathering tests have been carried out. The decay suffered by serpentinite slabs on the main façade of the Royal Chancery of Granada (Spain) has been used as the case study, using as well the original (quarry) serpentinites where the slabs come from, to understand the alteration evolution.

The mineral phases detected in the serpentinite's weathering material from the quarry are mainly hydrated iron and magnesium sulfates such as slavikite, rozenite, melanterite, pickeringite, halotrichite, or epsomite. These phases are weathering products of pre-existing phases, such as pyrite.

After the salt formation test, it was observed the presence of efflorescence, mainly composed of gypsum. Likewise, after the aging test in an acidic atmosphere, in addition to superficial alteration, the presence of efflorescence composed of hexahydrite, epsomite, or other hydrated sulfates was observed.

As for the serpentinites slabs in the main façade of the Royal Chancery, it was observed a notable increase in porosity and the presence of salts such as gypsum or epsomite. Several factors are considered to trigger the deterioration:

- The presence of sulfides, such as pyrite, in the serpentinite, plays a key role in the progress of decay. Its in situ oxidation and hydrolysis induce the formation of deleterious salts such as gypsum and epsomite.

- The incorrect restoration interventions using Portland cement and white marble provide an almost inexhaustible source of sulfates and calcium, accelerating the disintegration process. These anions and cations are dissolved by the water that penetrates through the porous system giving rise to the precipitation of gypsum and other salts.

- The studied serpentinites are emplaced in an urban environment, exposed to traffic, so that pollutant gasses such as SO_2 could also contribute to the deterioration of the stone. Such pollutant gases can react with water and atmospheric CO_2, generating an acidic medium that causes the dissolution of carbonates and serpentine minerals. In turn, this will result in the formation of sulfate salts. This phenomenon contributes to increase the amount of sulfates formed by the in situ weathering of sulfides present in the serpentinite.

- Upon sulfate precipitation and/or upon subsequent deliquescence/precipitation cycles (after RH and *T* fluctuation), crystallization pressure generation within the pores and microcracks of serpentine, results in the dramatic damage observed in the building.

- The above-mentioned decay processes are increased in the lower part of the building due to the greater contribution of water that the building has, mainly due to the capillary rise of underground water, summing up the proximity to a river bed, increasing the relative humidity of the area.

As a protection measure against future deterioration, it would be advisable, first, to eliminate all harmful material for the serpentinite, second, a desalination treatment and then consolidate the serpentinite with a compatible consolidant that also has protective (hydrophobic) properties (e.g., alkyl-alkoxysilane). Only if these actions do not solve the problem, it would be necessary to proceed to the replacement of the affected parts with new slabs coming from the same historical serpentinite quarry. If this is not possible due to administrative reasons, similar materials could be used, after a detailed study. It is also considered necessary to apply a suitable compatible mortar that reduces the possibility of salt formation when reacting with the serpentinite components. As

it does not seem possible to change the environmental conditions around the affected building, new treatments, like ultrafast laser surface texturing [74], could be tried on the serpentinite slabs to try to modify the wettability properties of the rock, to preserve the architectural heritage carver and/or built with serpentinite stone.

Acknowledgments

The University of Salamanca is acknowledged for the funding support to the Research Group CHARROCK. This research has been funded by the Spanish Government (grant CGL2015-70642-R), the European Commission (ERDF funds), the Junta de Andalucía (research group RNM-179), and the University of Granada (Unidad Científica de Excelencia UCE-PP2016-05). We also thank the personnel of the Centro de Instrumentación Científica (CIC; University of Granada) for assistance with FESEM-EDS analyses. This study was also financially supported by the Spanish Geological Survey (IGME).

Our sincere thanks go three anonymous reviewers for their useful comments and corrections to improve this paper.

Bibliography

[1] J.B. Moody, Serpentinization: a review, Lithos 9(2) (1976) 125-138. https://doi.org/10.1016/0024-4937(76)90030-X

[2] D.S. O'Hanley, Serpentinites: records of tectonic and petrological history, Oxford University Press, New York (US), 1996. https://doi.org/10.1017/S0016756897408257

[3] M.D. Pereira, M. Yenes, J.A. Blanco, M. Peinado, Characterization of serpentinites to define their appropriate use as dimension stone, in: R. Prikryl, B.J. Smith (Eds.), Building Stone Decay: From Diagnosis to Conservation, Geological Society, London, United Kingdom, 2007, pp. 55-62. https://doi.org/10.1144/GSL.SP.2007.271.01.06

[4] R. Navarro, D. Pereira, A. Gimeno, S. Del Barrio, Influence of natural carbonation process in serpentinites used as construction and building materials, Constr. Build. Mater. 170(10) (2018) 537-546. https://doi.org/10.1016/j.conbuildmat.2018.03.100

[5] M.C. Marchei, A. Sironi, R. Gnoli, Repertorio, in: G. Borghini (Ed.), Marmi antichi, Leonardo De Luca, Roma, 1989, pp. 131-302.

[6] V. Melfos, Green Thessalian stone: the byzantine quarries and the use of a unique architectural material from the Larisa area, Greece. Petrographic and geochemical characterization, Oxf. J. Archaeol 27 (2008) 387-405. https://doi.org/10.1111/j.1468-0092.2008.00313.x

[7] M.I. Gutiérrez-Deza, Revisión de dos pavimentos de opus sectile de Italica, Rómula 5 (2006) 149-166.

[8] J.M. Macias-Solé, J.J. Menchon-Bes, A. Muñoz-Melgar, I. Teixell-Navarro, La acrópolis de Tarraco y la implantación urbana del culto imperial en la capital de la Hispania Citerior, Bollettino di Archeologia on line Volume speciale A8(4) (2010) 50-66.

[9] J.A. Harrell, Survey of ornamental stones in mosques and other islamic buildings of the Pre-Ottoman Period In Cairo, Egypt, 2003. http://www.eeescience.utoledo.edu/faculty/harrell/Egypt/Mosques/Survey_Intro.htm. 2003 Accessed 05/13/2020.

[10] J.A. Harrell, M.A.T.M. Broekmans, D.I. Godfrey-Smith, The origin, destruction and restoration of colour in Egyptian travertine, Archaeom. 49(3) (2007) 421-436. https://doi.org/10.1111/j.1475-4754.2007.00312.x

[11] G. de Vecchi, M. Rossetti, S. Vannucci, La serpentina della Cattedrale di Santa Maria del Fiore a Firenze ed il suo degrado, in: G. Biscontin, D. Mietto (Eds.), Atti del Convegno Scienza e Beni Culturali: Le Pietre nell'Architettura: struttura e superfici, Bressanone, Lib. Progetto, Padua, 1991, pp. 247-256.

[12] A. Bralia, S. Ceccherini, F. Fratini, C. Manganelli Del Fà, M. Mellini, G. Sabatini, Anomaluos water absortion in low-grade serpentinites: more water than space?, Eur. J. Mineral. 7 (1995) 205-215. https://doi.org/10.1127/ejm/7/1/0205

[13] P. Malesani, E. Pecchioni, E. Cantisani, F. Fratini, Geolithology and provenance of materials of some historical buildings and monuments in the centre of Florence (Italy), Episodes 26(3) (2003) 250-255. https://doi.org/10.18814/epiiugs/2003/v26i3/017

[14] L. Marino, M. Corti, M. Coli, C. Tanini, C. Nenci, The "Verde di Prato" stones of cathedral and baptistery of Florence (abstract), in: E. Abbate, IUGS, European_Commission (Eds.) General Proceedings: 32nd International Geological Congress. Florence, Italy, August 20-28, 2004., Organizing Secretariat, Newtours, Florence, 2004.

[15] D. Gulotta, E. Bontempi, R. Bugini, S. Goidanich, L. Toniolo, The deterioration of metamorphic serpentinites used in historical architecture under atmospheric conditions, Q. J. Eng. Geol.Hydrogeol. 50 (2017) 402–411. https://doi.org/10.1144/qjegh2016-133

[16] A.P. Santo, E. Pecchioni, C.A. Garzonio, The San Giovanni Baptistery in Florence (Italy): characterisation of the serpentinite floor, IOP Conference Series: Materials Science and Engineering 364 (2018) 012069. https://doi.org/10.1088/1757-899X/364/1/012069

[17] J.L. Ruvalcaba, E. Melgar, T. Calligaro, Manufacturing analysis and non-destructive characterisation of green stone objects from the Tenochtitlan Templo Mayor Museum, Mexico, in: I. Turbanti-Memmi (Ed.) 37th International Symposium of Archaeometry, Springer, Siena, 2008, pp. 299-304.

[18] T.C. Meierding, Weathering of serpentine stone buildings in the Philadelphia region: a geographic approach related to acidic deposition, in: A.V. Turkington (Ed.), Stone decay in the architectural environment, Geological Society of America, Colorado (US), 2005, pp. 17-25.

[19] Stone Contact, International builders marketplace, 2020. https://www.stonecontact.com/stone/green-marble. 2020 Accessed 05/29/2020.

[20] R. Navarro, D. Pereira, C. Rodríguez-Navarro, E. Sebastian-Pardo, The Sierra Nevada serpentinites: the serpentinites most used in Spanish heritage buildings in: D. Pereira, B. Marker, S. Kramar, B. Cooper, B. Schouenborg (Eds.), Global Heritage Stone: Towards International Recognition of Building and Ornamental Stones, Geological Society, London (UK), 2015, pp. 101-108. http://dx.doi.org/10.1144/SP407.7

[21] A.A. Ruiz-Rodríguez, J.M. Gómez-Moreno Calera, I.M. Álamo Fuentes, Francisco del Castillo autor de la fachada de la Chancillería de Granada, Cuadernos del Arte 16 (1984) 159-172.

[22] M.T. Blanco-Varela, E. Menendez, M. Hoyos, Study of surface decay of the marbles and serpentine from the Descalzas Reales Convent at Madrid, in: D. Decrouez, J. Chamay, F. Zezza (Eds.) La conservation des monuments dans le bassin méditerranéen: actes du 2ème symposium international, Musee d'Art et d'Histoire-Geneve; Museum d'Histoire Naturelle, Geneva, 1991, pp. 167-175.

[23] F. Fratini, S. Ceccherini, E. Pecchioni, C. Manganelli del Fà, A. Scala, G. Galletti, Alterazione del marmo e della serpentinite costituenti il rivestimento della facciata della Collegiata di S. Andrea in Empoli (Firenze), in: G. Biscontin, D. Mietto (Eds.) Atti del Convegno Scienza e Beni Culturali: Le Pietre nell'Architettura: struttura e superfici, Bressanone, 1991, pp. 323-334.

[24] F. Cimmino, F. Faccini, A. Robbiano, Stones and coloured marbles of Liguria in historical monuments, Period. di Mineral 73 (2003) 71-84.

[25] M. Bastogi, F. Fratini, Geologia, litologia, cave e deterioramento delle pietre fiorentine, Memorie Descrittive della Carta Geologica d'Italia LXVI (2004) 27-42.

[26] M.D. Pereira, J.A. Blanco, M. Peinado, Study on serpentinites and the consequence of the misuse of natural stone in buildings for construction, J. Mater. Civ. Eng. 25(10) (2013) 1563–1567. https://doi.org/10.1061/(ASCE)MT.1943-5533.0000689

[27] M.D. Pereira, M. Peinado, J.A. Blanco, M. Yenes, Geochemical characterization of serpentinites at Cabo Ortegal, northwestern Spain, Can. Mineral. 46 (2008) 317-327. https://doi.org/10.3749/canmin.46.2.317

[28] M.D. Pereira, M. Peinado, M. Yenes, S. Monterrubio, J. Nespereira, J.A. Blanco, Serpentinites from Cabo Ortegal (Galicia, Spain): a search for correct use as ornamental stones, in: R. Prikryl, A. Török (Eds.), Natural stone resources for historical monuments, Geological Society, London (UK), 2010, pp. 81-85. https://doi.org/10.1144/SP333.8

[29] J.A. Harrell, Stones in ancient Egypt, 2009. http://www.eeescience.utoledo.edu/egypt/. 2009 Accessed 05/13/2020.

[30] I. Ismael, M. Hassan, Characterization of some egyptian serpentinites used as ornamental stones, Chin. J. Geochem. 27(2) (2008) 140-149. https://doi.org/10.1007/s11631-008-0140-0

[31] R. Navarro, L. Catarino, D. Pereira, F.P.S.C. Gil, Effect of UV radiation on chromatic parameters in serpentinites used as dimension stones, Bull. Eng. Geol. Environ. 78(7) (2019) 5345-5355. https://doi.org/10.1007/s10064-019-01469-3

[32] R. Navarro, D. Pereira, A. Gimeno, S. del Barrio, Caracterización mineralógica y físico-mecánica de las serpentinitas de la comarca de Macael (Almería, S de España) para su uso como roca ornamental., Geogaceta 54 (2013) 47-50.

[33] R. Navarro, D. Pereira, A. Gimeno, S. del Barrio, Characterization of the natural variability of Macael serpentinite (Verde Macael) (Almería, south of Spain) for their appropriate use in the building industry, in: G. Lollino, A. Manconi, F. Guzzetti, M. Culshaw, P. Bobrowsky, F. Luino (Eds.), Engineering geology for society and territory. Volume 5: urban geology, sustainable planning and landscape exploitation, Springer International Publishing AG, Switzerland, 2015, pp. 209-211. https://doi.org/10.1007/978-3-319-09048-1_40

[34] J. Nespereira, R. Navarro, S. Monterrubio, M. Yenes, D. Pereira, Serpentinite from Moeche (Galicia, North Western Spain). A Stone Used for Centuries in the Construction of the Architectural Heritage of the Region, Sustainability 11(9) (2019) 2700. https://doi.org/10.3390/su11092700

[35] R. Navarro, M.D. Pereira, A. Gimeno, S. Del Barrio, Verde Macael: a serpentinite wrongly referred to as a marble, Geosci. 3(1) (2013) 102-113. https://doi.org/10.3390/geosciences3010102

[36] C. Sanz de Galdeano, A.C. López Garrido, The Nevado-Filábride Complex in the western part of Sierra de los Filabres (Betic Internal Zone), structure and lithologic succession, Bol. Geol. Min. 127(4) (2016) 823-836. https://doi.org/10.21701/bolgeomin.127.4.005

[37] E. Puga, M. Fanning, A. Díaz de Federico, J.M. Nieto, L. Beccaluva, G. Bianchini, M.A. Díaz-Puga, Petrology, geochemistry and U–Pb geochronology of the Betic Ophiolites: Inferences for Pangaea break-up and birth of the westernmost Tethys Ocean, Lithos 124(3-4) (2011) 255-272. https://doi.org/10.1016/j.lithos.2011.01.002

[38] J.A. Vera, Cordillera Bética y Baleares, in: J.A. Vera (Ed.), Geología de España, Sociedad Geológica de España (S.G.E.)-Instituto Geológico y Minero de España (I.G.M.E.), Madrid, 2004, pp. 345-464.

[39] J.D. Martín-Ramos, Using XPowder©, A Software Package for Powder X-Ray Diffraction Analysis D.L.GR-1001/04, Spain, 1-105, J. Daniel Martin, Granada, 2004.

[40] UNE-EN 13919, Métodos de ensayo para la piedra natural. Determinación de la resistencia al envejecimiento por la acción de SO2 en presencia de humedad, Asociación Española de Normalización y Certificación (AENOR), Madrid, 2003.

[41] A. Luque, M.V. Martínez de Yuso, G. Cultrone, E. Sebastián-Pardo, Analysis of the surface of different marbles by X-ray Photoelectron Spectroscopy (XPS) to evaluate decay by SO2 attack, Environ. Earth Sci. 68 (2013) 833-845. https://doi.org/10.1007/s12665-012-1786-9

[42] D.L. Whitney, B.W. Evans, Abbreviations for names of rock-forming minerals, Am. Mineral. 95 (2010) 185–187. https://doi.org/10.2138/am.2010.3371

[43] F.J. Wicks, E.J.W. Whittaker, Serpentinite textures and serpentinization, Can. Mineral. 15 (1977) 459-488.

[44] O.R. Eckstrand, The Dumont serpentinite; a model for control of nickeliferous opaque mineral assemblages by alteration reactions in ultramafic rocks (in an issue devoted to Canadian mineral deposits), Econ. Geol. 70 (1975) 183-201. https://doi.org/10.2113/gsecongeo.70.1.183

[45] B.R. Frost, On the stability of sulfides, oxides and native metals in serpentinites, J. Petrol. 26 (1985) 31-63. https://doi.org/10.1093/petrology/26.1.31

[46] J.P. Lorand, Mineralogy and chemistry of Cu–Fe–Ni sulfides in orogenic-type spinel peridotite bodies from Ariege (northeastern Pyrenees, France), Contrib. Mineral. Petrol. 103 (1989) 335-345. https://doi.org/10.1007/BF00402920

[47] J.C. Alt, W.C. Shanks, Sulfur in serpentinized oceanic peridotites: Serpentinization processes and microbial sulfate reduction, J. Geophys. Res. [Solid Earth] 103(B5) (1998) 9917-9929. https://doi.org/10.1029/98JB00576

[48] F. Klein, W. Bach, Fe–Ni–Co–O–S phase relations in peridotite–seawater interactions, J. Petrol. 50(1) (2009) 37-59. https://doi.org/10.1093/petrology/egn071

[49] J.C. Alt, C.J. Garrido, W.C. Shanks III, A. Turchyn, J.A. Padrón-Navarta, V. López Sánchez-Vizcaíno, M.T. Gómez-Pugnaire, C. Marchesi, Recycling of water, carbon, and sulfur during subduction of serpentinites: A stable isotope study of Cerro del Almirez, Spain, Earth Planet. Sci. Lett. 327-328 (2012) 50-60. https://doi.org/10.1016/j.epsl.2012.01.029

[50] R. Arana-Castillo, Investigaciones mineralógicas en Sierra Nevada (Cordilleras Béticas), PhD. Thesis, University of Granada, Granada (Spain), 1973, p. 547

[51] J.L. Jambor, D.K. Nordstrom, C.N. Alpers, Metal-sulfate salts from sulfide mineral oxidation, Rev. Mineral. Geochem. 40(1) (2000) 303-350. https://doi.org/10.2138/rmg.2000.40.6

[52] D.K. Nordstrom, C.N. Alpers, Geochemistry of acid mine waters, in: G.S. Plumlee, M.J. Logsdon (Eds.), The environmental geochemistry of mineral deposits. Part A: processes, techniques and health issues, Society of Economic Geologists, 1999, pp. 133-160.

[53] J.W. Anthony, R.A. Bideaux, K.W. Bladh, M.C. Nichols, Handbook of mineralogy, 2011. http://www.handbookofmineralogy.org/. 2011 Accessed 05/29/2020.

[54] S. Dimitrova, V. Mladenova, L. Hecht, Efflorescent sulfate crystallization on fractured and polished colloform pyrite surfaces: a migration pathway of trace elements, Minerals 10(1) (2020) 12. https://doi.org/10.3390/min10010012

[55] P.C. Singer, W. Stumn, Acidic mine drainage: the rate-determining step, Science 167 (1970) 1121-1123. https://doi.org/10.1126/science.167.3921.1121

[56] C.J. Ritsema, J.E. Groenenberg, Pyrite oxidation, carbonate weathering, and gypsum formation in a drained potential acid sulfate soil, Soil Sci. Soc. Am. J. 57(4) (1993) 968-968. https://doi.org/10.2136/sssaj1993.03615995005700040015x

[57] M. Schiro, E. Ruiz-Agudo, C. Rodriguez-Navarro, Damage mechanisms of porous materials due to in-pore salt crystallization, Phys. Rev. Lett. 109(26) (2012) 265503. https://doi.org/10.1103/PhysRevLett.109.265503

[58] P. Lopez-Arce, E. Doehne, W. Martin, S. Pinchin, Sales de sulfato magnésico y materiales de edificios históricos: simulación experimental de laminaciones en calizas mediante ciclos de humedad relativa y cristalización de sales, Mater Construcc. 58(289-290) (2008) 125-142. https://doi.org/10.3989/mc.2008.v58.i289-290

[59] M. Steiger, K. Linnow, H. Juling, G. Gülker, A.E. Jarad, C. Von Ossietzky, S. Brüggerhoff, D. Kirchner, Hydration of $MgSO_4*H_2O$ and generation of stress in porous materials, Cryst. Growth Des. 8(1) (2008) 336–343. https://doi.org/10.1021/cg060688c

[60] A.E. Charola, J. Pühringer, M. Steiger, Gypsum: a review of its role in the deterioration of building materials, Environ. Geol. 52(2) (2007) 339-352. https://doi.org/10.1007/s00254-006-0566-9

[61] I.M. Chou, R.R. Seal II, B.S. Hemingway, Determination of melanterite-rozenite and chalcanthite-bonattite equilibria by humidity measurements at 0.1 MPa, Am. Mineral. 87(1) (2002) 108-114. https://doi.org/10.2138/am-2002-0112

[62] C. Rodríguez-Navarro, E. Doehne, Salt weathering: influence of evaporation rate, supersaturation and crystallization pattern, Earth Surf. Processes Landforms 24(3) (1999) 191-209. https://doi.org/10.1002/(SICI)1096-9837(199903)24:3<191::AID-ESP942>3.0.CO;2-G

[64] G.W. Scherer, Crystallization in pores, Cement Concrete Res. 29(8) (1999) 1347-1358. https://doi.org/10.1016/S0008-8846(99)00002-2

[65] G.W. Scherer, Stress from crystallization of salt, Cement Concrete Res. 34(9) (2004) 1613-1624. https://doi.org/10.1016/j.cemconres.2003.12.034

[66] E. Ruiz-Agudo, F. Mees, P. Jacobs, C. Rodriguez-Navarro, The role of saline solution properties on porous limestone salt weathering by magnesium and sodium sulfates, Environ. Geol. 52 (2007) 269–281. https://doi.org/10.1007/s00254-006-0476-x

[67] C. Rodriguez-Navarro, E. Sebastian, Role of particulate matter from vehicle exhaust on porous building stones (limestone) sulfation, Sci. Total. Environ. 187(2) (1996) 79-91. https://doi.org/10.1016/0048-9697(96)05124-8

[68] J. Simao, E. Ruiz-Agudo, C. Rodríguez-Navarro, Effects of particulate matter from gasoline and diesel vehicle exhaust emissions on silicate stones sulfation, Atmos. Environ. 40 (2006) 6905-6917. https://doi.org/10.1016/j.atmosenv.2006.06.016

[69] S. Yu, C.T. Oguchi, Role of pore size distribution in salt uptake, damage, and predicting salt susceptibility of eight types of Japanese building stones, Eng. Geol. 115 (2010) 226-236. https://doi.org/10.1016/j.enggeo.2009.05.007

[70] C. Noiriel, F. Renard, M.L. Doan, J.P. Gratier, Intense fracturing and fracture sealing induced by mineral growth in porous rocks, Chem. Geol. 269(3-4) (2010) 197-209. https://doi.org/10.1016/j.chemgeo.2009.09.018

[71] S. Teir, H. Revitzer, S. Eloneva, C.J. Fogelholm, R. Zevenhoven, Dissolution of natural serpentinite in mineral and organic acids, Int. J. Miner. Process. 83(1-2, 4) (2007) 36-46. https://doi.org/10.1016/j.minpro.2007.04.001

[72] J.W. Morse, R.S. Arvidson, The dissolution kinetics of major sedimentary carbonate minerals, Earth Sci. Rev. 58 (2002) 51-84. https://doi.org/10.1016/S0012-8252(01)00083-6

[73] V. Vergès-Belmin, Illustrated glossary on stone deterioration patterns, Monuments & Sites, ICOMOS-ISCS, Paris, 2008, p. 86.

[74] M. Urosevic, E.M. Sebastián-Pardo, E. Ruiz-Agudo, C. Cardell, Physical properties of carbonate rocks used as a modern and historic construction material in Eastern Andalusia, Spain, Mater Construcc. 61(301) (2011) 93-114. https://doi.org/10.3989/mc.2011.v61.i301

[75] A.J. López, A. A. Ramil, J.S. Pozo-Antonio, T. Rivas, D. Pereira, Ultrafast laser surface texturing: a sustainable tool to modify wettability properties of marble, Sustainability 11(15)

(2019) 145-161. https://doi.org/10.3390/su11154079